Int. J. Multiphase Flow Vol. 19, No. 6, pp. 943–964, 1993
Printed in Great Britain.

0301-9322/93 $6.00 + 0.00

NUCLEATION AND FLASHING IN NOZZLES—1

A DISTRIBUTED NUCLEATION MODEL

T. S. SHIN† and O. C. JONES‡
Department of Nuclear Engineering and Engineering Physics and Center for Multiphase Research, Rensselaer Polytechnic Institute, Troy, NY, U.S.A.

(Received 20 December 1990; in revised form 30 August 1993)

Abstract—It is well known that both the number and size of bubbles must be accurately determined for the initial calculation of flashing void development downstream of flashing inception in ducts, nozzles and restrictions. This paper presents a new method of accurately determining both for small geometries with water, which results in accurate calculation of the downstream void development. A wall cavity model is described for use in the calculation of nucleation rates and bubble number densities at flashing inception, and subsequently in the calculation of the void development downstream of minimum area zones in nozzles. The model is based on the physics of the nucleation phenomena in flashing and considers transient conduction to be the sole means of heat transfer from the superheated liquid to the vapor bubble. The activation criterion developed for site nucleation is one-sided, due to the uniform superheat, rather than two-sided as in boiling. A figure of merit for the particular fluid solid combination is then determined which yields the minimum nucleation surface energy per site. Characteristic site nucleation frequencies and the number densities of nucleation sites of given sizes are then obtained from the data, providing the first link between a surface-characteristic-based nucleation and evaporation model and global behavior. Throat void fractions for all data found in the literature are $<1\%$, confirming earlier assumptions. A bubble transport equation is used to predict the number density and size of bubbles at the throat. Throat superheats are then calculated for all throat superheats up to ~ 100 K and expansion rates between 0.2 bar/s to over 1 Mbar/s, with a standard deviation of 1.9 K. This extends previous correlations by more than 3 orders of magnitude. As a result, flow rates can be calculated to within 3% of measured values using a combination of single-phase theory and accurate calculation of the throat pressure under critical conditions. This provides a valuable consistency check to independent critical flow predictions.

Key Words: critical flow, nucleation, bubble growth, bubble number density, cavities, vapor generation, interfacial area

1. INTRODUCTION

The discharge rate of subcooled liquids from pressurized containers is of interest in many situations which apply to the safety of chemical, process and nuclear equipment. Critical flow phenomena limit the discharge rates, but the analysis of critical flow rate becomes difficult due to both mechanical and thermal nonequilibrium effects. An accurate knowledge of flashing phenomena is essential in the determination of critical flow rate and, thus, for such things as cooling inventory or forces on piping and vessels. Accurate calculation of flashing has been previously shown to be the key to predicting such discharges when the inlet flows are subcooled (Abuaf *et al.* 1980, 1983). While the critical condition may not occur at the throat in two-phase evaporative flows, it is useful to utilize this location for calculational purposes, and this has been the general practice.

"Flashing inception" is usually taken to mean the start of significant void development, much in the same manner as the net vapor generation (NVG) point is considered in boiling. Abuaf *et al.* (1981) showed that the flashing inception of initially subcooled liquids was experimentally observed to be confined to regions very close to the throat. Single-phase calculations thus gave critical flow rates within a few percent. No theoretical explanation for these observations, however, was available and only the models of Alamgir & Leinhard (1981) and Jones (1980) were available to predict "inception" superheat, thus giving throat pressures.

Both the initial size and number density of the bubbles, or the equivalent, are needed to provide closure for calculations of void development downstream of the throat in nozzles (cf. Malnes 1975; Rohatgi & Reshotko 1975; Wolfert 1976; Ardron 1978; Aguilar & Thompson 1981). Typical past

†Present address: Combustion Engineering, Windsor Locks, CT, U.S.A.
‡Author for correspondence.

practice was to provide an estimate of the initial void fraction (typically $\ll 1\%$) and number density (typically 10^8–$10^{13}\ m^{-3}$). Resultant void growth calculations have not been in good agreement with existing data in either trends or magnitude.

It is the purpose of this paper to describe a composite model for continuous nucleation in the superheated zone upstream of the throat for single-component liquids with particular reference to water systems. This model will utilize fundamental physical principals together with empiricism where necessary. For the first time in the phase-change literature, a method is given for coupling the basic thermofluid descriptions of surface-cavity-based bubble nucleation with the global flow parameters such as superheat, void fraction, pressure loss and flow rates. It will be shown in the companion paper (Blinkov *et al.* 1993, this issue, pp. 965–986) that these results lead to reasonable calculations of void development downstream.

2. BACKGROUND

Flashing Inception and Critical Flows

Early literature reviews of the critical discharge of flashing flows were presented by Saha (1978) and by Hsu (1972). Homogeneous equilibrium models were shown to underpredict critical discharge rates for short pipes and near saturation or subcooled upstream conditions due to the liquid superheat and resultant underprediction of void fraction. Abdollahian *et al.* (1982) reviewed two-phase critical flow models varying in complexity from simple correlation-type models to complex two-fluid models.

Many experiments have been undertaken with critical flow in nozzles and orifices. Bailey (1951) conducted one of the earliest experiments to investigate the metastability of initially subcooled water, finding only small superheats. Brown (1961) and Schrock *et al.* (1977) later observed throat superheats up to nearly 100°C, reporting pressure profiles and critical flow rates. They noted that both the number and size of bubbles are needed for prediction.

Powell's (1961) subcooled-inlet critical flow data, having only inlet and exit pressures and inlet temperatures, remained poorly predicted until Abuaf *et al.* (1980, 1983) obtained data indicating negligible throat void fraction and predicted the data base on the throat superheat model of Alamgir & Lienhard (1981).

Simpson & Silver (1962) used a kinetically-derived nucleation rate model along with the Plesset & Zwick (1954) bubble growth model to calculate flashing critical flows. This model gave good agreement at small superheat but diverged from experimental data at large superheat.

Edwards (1968) used a conduction-controlled bubble growth law at constant superheat and constant pressure to formulate the mechanism of vapor generation during depressurization but needed to make an assumption regarding initial sizes and number densities.

A slip flow model was developed by Moody (1966) but it is based on thermodynamic equilibrium. Its simplicity has resulted in its widespread usage in nuclear safety analysis and it provides a reference prediction of critical flow rate for many two-phase flow conditions.

Henry & Fauske (1971) accounted for nonequilibrium effects at the choking plane as $x = Nx_e$, where x_e is the equilibrium, thermodynamically-derived quality, x is the actual quality and N a parameter. They matched their results well with the experiments for qualities $>1\%$ but it was later found that N needed to be adjusted to predict other results such as the 1979 Marviken critical flow data (EPRI 1979) adequately. A similar approach was used by Bauer *et al.* (1976).

Jones & Saha (1977), Riebold *et al.* (1981) and Jones (1982) have subsequently shown that the linear relationship suggested by Henry & Fauske (1971) makes the *de facto* assumption that the rate of change of the actual quality with equilibrium quality is a constant, contrary to results obtained from basic mass conservation and neglecting the real relaxation phenomena. Fluids in thermal nonequilibrium tend toward the equilibrium state at rates governed by the interfacial processes, independent of the equilibrium path driving the phase change.

Sozzi & Sutherland (1975) found that geometry played an important role in critical flow phenomena, particularly for short nozzles. Critical mass flux was observed to decrease with increasing throat diameter.

Malnes (1975) used a conduction-controlled bubble growth law similar to Simpson & Silver

(1962). Two dimensionless empirical constants were needed for data prediction. Those obtained based on the data of Henry *et al.* (1970), however, did not predict well the data of Fauske (1964).

Rohatgi & Reshotko (1975) also used a method similar to that of Simpson & Silver (1962), again needing two unknown parameters for closure which they determined from experimental data. Simoneau's (1975) nitrogen experiments were predicted by choosing a nucleation site density of about $10^6\,m^3$.

Fritz *et al.* (1976) pointed out that the bubble number density was the most uncertain factor in their model. They recommended bubble number densities between 10^8 and $2 \times 10^{10}\,m^{-3}$ for water temperatures of 250–325°C.

Wolfert (1976) again found that two independent parameters needed to be chosen to make comparisons with the data. Different data required different initial void fractions and number densities of bubbles. Values of the order of $10^9\,m^{-3}$ for number densities were chosen together with a minimum void fraction of 10^{-6}, corresponding to a minimum bubble diameter of 7.2 mm.

Aguilar & Thompson (1981) used number density and superheat as the two independent parameters and chose $10^9\,m^{-3}$ as the bubble density. Constant superheat did not adequately predict the nonequilibrium flashing in rapid depressurization.

Ardron (1978) also introduced a nucleation model based on the kinetic theory and used a simple growth rate model for bubbles. The two empirical factors they chose were nucleation superheat (3°C) and nucleation site density ($10^6\,m^{-3}$).

Winters & Merte (1979) formulated a model that treated the expanding two-phase fluid as a pseudo-homogeneous mixture of uniformly distributed, heat transfer dominated, spherical vapor bubbles surrounded by superheated liquid. Poor agreement was obtained with this critical flow data.

Zimmer *et al.* (1979) reported carefully controlled, degassed, steady flow experiments with detailed pressure and two-dimensional void profiles. Flashing inception superheats were found to be important in determining void development downstream of the inception point. For the first time, void data were obtained showing negligible voids at the throat.

Rivard & Travis (1980) based their model on a description of turbulence-enhanced, thermal diffusivity in the liquid and a Weber number criterion for bubble size. They chose an initial void fraction of 2×10^{-4} and an initial bubble number density of $10^9\,m^{-3}$, which resulted in an initial bubble diameter of $7.2 \times 10^{-5}\,m$. The calculated critical flow rate deviated from the Semiscale blowdown tests by up to 20% shortly after the initiation of blow-down.

Richter (1981) introduced a two-fluid model which required assumption of an initial bubble size and a fixed nucleation site density at the onset of flashing. He chose an initial bubble number density of $10^{11}\,m^{-3}$ and an initial bubble diameter of $2.5 \times 10^{-5}\,m$. Marviken test data were adequately predicted but prediction of other data such as that of Reocreux (1976) required adjustments.

Celata *et al.* (1982) investigated the critical flow of subcooled liquid through different channels. They reported data on the critical mass flow rate at different degrees of inlet subcooling and static pressure profile along the channel.

While the previously described research utilized water-based systems, several works on flashing phenomena with cryogenic liquids in a converging–diverging nozzle were reported by Simoneau (1975) and by Hendricks *et al.* (1976). Their data included the axial pressure distribution along the nozzle and the critical flow rates for various subcooled inlet conditions. They found that the fluid appears to be a metastable liquid upstream of the throat and that no model adequately describes the whole range of the experiment.

The matter of initial superheats was first examined by Alamgir & Lienhard (1981) who developed a semi-empirical correlation motivated by classical nucleation theory to predict the pressure undershoot at the onset of flashing below the saturation pressure during a rapid depressurization in water covering the range from 0.004 to 1.8 Mbar/s. Jones (1980) then incorporated this model into a Lagrangian description of flowing decompression in pipes and nozzles to include the effects of turbulence, but did not extend the dynamic decompression range.

Abuaf *et al.* (1980, 1983) utilized a combination of the Alamgir–Lienhard and Jones approaches to determine the superheats at the throat in nozzles. They hypothesized that void development upstream of the throat was negligible. Critical flow rates were then based on single-phase flow

equations using the throat pressure taken based on the predicted superheat. Results were within 5% of the experimental values for a wide range of experiments reported in the literature.

Saha *et al.* (1981) developed a model for the net vapor generation rate in each flow regime downstream of the throat. The bubble number density and initial void fraction at the flashing inception point were varied to obtain optimum fits with the void fraction data. The model also required *a priori* knowledge of the liquid superheat at flashing inception to obtain reasonable agreement with Zimmer *et al.*'s (1979) data for void fractions $<20\%$.

Levy & Abdollahian (1982) used a slight modification to the Alamgir–Lienhard correlation based on the data of Reocreux (1976) and Zimmer *et al.* (1979). Their final expression for the critical flow rate was virtually identical to those proposed by both Abuaf *et al.* (1980, 1983) and Fincke *et al.* (1981).

Schrock & Amos (1984) conducted experiments for flashing flows through slits. They found that the inhomogeneous equilibrium (IHE) model predicted the measured mass flux quite well in spite of considerable underprediction of the exit pressure. They also found the prediction of Alamgir & Lienhard (1981) for flashing inception to be quite inaccurate in some cases, but no reasons were given.

Summary of the flashing literature

In general, most models failed in the prediction of critical flow rates outside the data base utilized for setting parameters in the correlation. Critical flow data for initially subcooled flows data up to about 1981 had one thing in common: flow rates are consistently higher than predictions based on equilibrium theory. The consensus was that to account for the observations significant thermal nonequilibrium must be present, yielding significant liquid superheat and much less void development than equilibrium values would suggest. Predictions of throat superheat improved calculations of critical flows but did little to advance the understanding of the process.

Analyses of these situations required two independent parameters at the "start" of the flashing process. These parameters generally were the equivalent of the initial bubble number density and size. All bubble growth models used were applicable only to uniformly superheated liquids. Jones & Zuber (1978), however, demonstrated that the constant pressure theories of Plesset & Zwick (1954), Forster & Zuber (1954) and Scriven (1959) failed when applied to the transient pressure field.

All early modeling efforts assumed that the bubbles become uniformly distributed in the flow regardless of the nucleation site, but no consensus exists on the location or distribution of the heterogeneous nucleation sites. Simpson *et al.* (1962), Rohatgi & Reshotko (1975), Malnes (1975) and Ardron (1978) all assumed that heterogeneous nucleation sites occur in the bulk fluid. However, the BNL experimental work of Zimmer *et al.* (1979) and Abuaf *et al.* (1981) showed conclusively that the important nucleation sites are at the perimeter of the channel, at least for small ducts. That this is generally the case in all geometries, however, has not yet been shown and indeed, is quite open to question.

Nucleation

Numerous studies have been undertaken with bubble nucleation on the surface in boiling. Among them, Bankoff (1958) studied the theoretical thermodynamic aspects of the nucleation process. He found that the free energy difference required for nucleation in a solid phase can be smaller than, equal to or larger than that for the homogeneous phase, depending on whether the solid geometry is a cavity, a perfect flat or a protruding point.

Later, Hsu (1962) analyzed the physics of bubble nucleation from cavities by using a model of Hsu & Graham (1961). Hsu postulated that bubble growth from an incipient nucleation site would begin when the whole surface of the hemispherical bubble surmounting this site was at a temperature greater than the equilibrium temperature corresponding to a bubble of that radius. His simplified nucleation criterion for boiling was found to agree with the experimental results of Clark *et al.* (1965) and Griffith & Wallis (1959). The early work of Bankoff, and the following work by Hsu formed the foundation of present concepts of boiling bubble-formation phenomena.

Han & Griffith (1965) proposed a similar nucleation criteria to Hsu's except that the constant

was altered. Both of the proposed models for nucleation require knowledge of the thermal boundary layer thickness. These models were verified qualitatively by Bergles & Rohsenow (1962).

Shoukri & Judd (1978) developed a theoretical model for bubble departure frequency in boiling as a function of the cavity radius as well as the wall superheat and liquid subcooling. In their model, the time variations of the wall temperature through the bubble cycle are incorporated.

Jones & Shin (1986) used Hsu's concept but showed that nucleation at cavities in uniform superheat had somewhat different physics than that in boiling. They developed a one-sided nucleation activation criterion for such cases. Shin & Jones (1988) then reported on the use of this activation criterion together with a method which allowed characteristic cavity values for a given surface to be obtained. The result provided the first method of coupling active cavity considerations to a nucleating surface to obtain bubble number densities.

Kocamustafaogullari & Ishii (1983) developed a model to describe the nucleation site density in subcooled boiling in dimensionless terms. They used the Fritz (1935) departure size for bubbles and Zuber's (1963) bubble departure frequency, recognizing their dubious value in this application. In their case the wall nucleation rate is proportional to the 4.4 power of the local wall superheat. This correlation was utilized in an attempt to predict the nucleation site density in flashing systems (Jones & Shin 1984) and the resultant void distribution. It was found, however, that the resultant nucleation rates were significantly lower than those needed to obtain proper predictions. It was this finding which led to the present realization that nucleation in subcooled boiling and that in flashing were sufficiently different to require separate consideration.

Review Summary

Up until quite recently, then, the general state of knowledge relating to the flashing of initially subcooled liquids was as follows:

1. The general consensus is that thermal nonequilibrium plays a strong role in the behavior of flashing of initially subcooled liquids in nozzles.
2. Numerous models for nucleation inception have been suggested. None have been found to be adequate and all, generally, were found to rely on two or more empirical estimates, such as bubble number density and initial void fraction. None have any general validity.
3. The initial flashing process has been largely treated as an inception phenomenon. Little has been done to consider the distribution of nucleation over the entire superheated region, even though it is well known that this is actually the case.
4. The flashing zone in nozzles is confined in practice to a region very close to the location of minimum pressure. No adequate explanation for this behavior exists.
5. The process of nonequilibrium vapor generation is an initial-value path-dependent process. Description of the initial value or initiation of this process has yet to be determined on other than an *ad hoc* basis.
6. No coupling has yet been made between the thermophysical description of bubble nucleation and growth at a surface cavity and the global flow parameters such as superheat, void fraction, pressure loss and flow rates.
7. Nucleation processes in subcooled boiling and those in flashing represent basically different physical processes needing different mathematical descriptions.

3. ANALYSIS

The transition from liquid to a two-phase mixture through pipes and nozzles by flashing usually takes place in several stages. Initially subcooled liquid encounters a region of decreasing pressure which may depend on acceleration and/or friction (figure 1) and is brought to a saturated state. A further decrease in pressure causes the liquid to become superheated. As liquid superheat is obtained, bubble nucleation starts, slowly at first and then more rapidly as the superheat increases. The nucleation rate is a strong function of the thermodynamic state of the superheated liquid, sometimes varying by orders of magnitude over very small temperature spans.

Nucleation rates will first increase to a maximum value. Nucleation has been shown to occur

on solid boundaries, at least in laboratory situations, and so heterogeneous wall nucleation shall be the mode considered herein. It is expected that the nucleation rate will subsequently decrease due to evaporative cooling of the liquid boundary layers adjacent to solid surfaces. In this respect it is similar to the formation of condensation nuclei in shock tubes (Wegener 1969, 1975). The net result is a limited nucleation zone, wherein virtually all the bubbles which go into the subsequent void development process are formed.

Following the nucleation zone, bubbles will grow as they flow downstream, generally limited by conduction processes at liquid–vapor interfaces. It is expected that spherical bubble growth processes will dominate void development in the early stages of the process, and perhaps up to quite high void fractions owing to the rapid transport times and the limited times available for bubble agglomeration in high-speed flows. This problem will be treated in the companion paper (Blinkov *et al.* 1993).

The analysis of this problem, therefore, will be broken up into three stages:

1. Nucleation, growth and departure at a single cavity.
2. Overall nucleation zone and bubble transport to the throat.
3. Void development downstream of the throat.

The first two will be discussed in turn. The third will be the subject of the companion paper (Blinkov *et al.* 1993). Single-cavity nucleation theory in uniform superheat has been reported previously (Jones & Shin 1986) as well as the use of this theory for calculating continuous nucleation in the superheated upstream of the throat in nozzles (Shin & Jones 1987). These will only be summarized herein.

Single-cavity Nucleation

Cavity activation

The first problem is to develop a criterion for determining when cavities are active. Consider the differences between flashing and boiling. One major difference is the way in which the thermal layers adjacent to the walls behave. As shown in figure 2(a), the wall layer in subcooled boiling is superheated and a bubble at a cavity would be stable and support growth if it were completely confined in the superheated layer (Hsu's criterion).

For flashing [figure 2(b)], the liquid is uniformly superheated away from the cavity. At the cavity

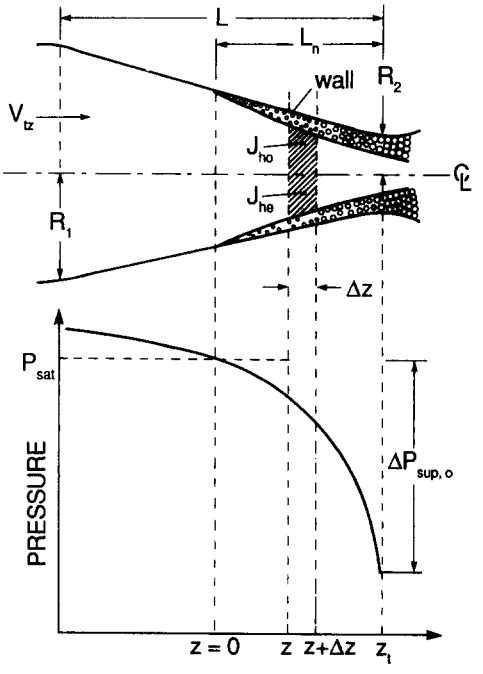

Figure 1. Schematic of the nucleation zone in a converging nozzle.

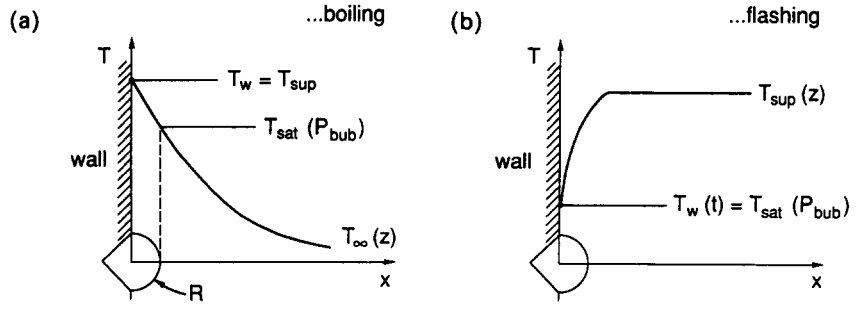

Figure 2. Stability criteria for cavity nuclei: (a) subcooled boiling; (b) flashing.

during growth, the wall drops to saturation and then recovers as the wall and liquid start to equilibrate following departure of the vapor nucleus. The equivalent to Hsu's nucleation criterion for flashing is that a stable bubble will nucleate when the wall temperature increases to the saturation temperature inside a bubble of radius identical to that of the cavity.

An expression for the transient liquid temperature, and hence the contact-line temperature following departure, can be determined by analyzing the combined fluid–solid conduction problem at a nucleation site but ignoring the geometry of the site itself. The following assumptions are made:

1. The problem is one-dimensional and the actual cavity geometry is ignored.
2. The properties of the liquid and solid are constant.
3. There is no contact resistance between the solid and liquid.
4. The liquid and solid are semi-infinite and stationary.
5. The liquid has uniform superheat far from the solid.
6. Convection of the liquid is negligible.

The problem is broken up into two intervals: bubble growth period to departure; dwell time between departure and nucleation. A detailed solution to this problem may be found in Jones & Shin (1986).

Stage 1—growth period. During this time, the vapor temperature inside the bubble, and hence at the vapor–solid interface, is at the saturation temperature according to the internal bubble pressure. It is assumed that this pressure decreases rapidly and has a value characteristic to that according to the local liquid pressure. The wall temperature, then, is assumed to start at uniform superheat and undergo an instanteous decrease to the local saturation temperature. The solution to this problem is well known to be

$$\frac{T_s(y,t)-T_{sat}}{T_{sup}-T_{sat}}=\frac{T_s-T_{sat}}{\Delta T_{sup}}=\mathrm{erf}\left(\frac{-y}{2\sqrt{\alpha_s t}}\right), \qquad [1]$$

where the distance into the solid, y, is negative; T is temperature with the subscripts s representing the solid, sat representing the saturated state in the liquid and sup representing the superheated state in the liquid, ΔT_{sup} is the positive value of the liquid superheat, α_s is thermal diffusivity of the solid and t is time. Of course the assumption implies the wall equilibrates towards the superheat temperature during the dwell times and towards the local saturation temperature inside a large bubble during growth periods, and is strictly applicable only to the case where the dwell and growth times are "sufficiently" long.

Stage 2—dwell period. During this period, which begins with bubble departure, uniformly superheated liquid impacts the solid, an interfacial contact temperature is established and both liquid and solid begin to equilibrate towards the uniform superheat temperature of the bulk liquid.

The solution to stage 1 will provide the initial conditions for the solution to this stage. In this case, both liquid and solid are considered with one-dimensional conduction equations for each. The problem to be solved is thus

$$\frac{\partial^2 T_s}{\partial y^2}=\frac{1}{\alpha_s}\frac{\partial T_s}{\partial t} \quad \text{and} \quad \frac{\partial^2 T_L}{\partial y^2}=\frac{1}{\alpha_L}\frac{\partial T_L}{\partial t}, \qquad [2]$$

subject to the initial conditions (at $t = 0$, for $y < 0$)

$$T_s(y, 0) = T_{sat} + \Delta T_{sup} \operatorname{erf}\left(\frac{-y}{2\sqrt{\alpha_s t_g}}\right), \quad [3]$$

where t_g is the growth time of the precursor bubble. Boundary conditions require that the fluid and solid temperature match at the interface so that, with the subscript L representing the liquid,

$$\text{at } y = 0, \quad T_s(0, t) = T_L(0, t), \quad [4]$$

and also the heat flux, so that

$$\text{at } y = 0, \quad k_s \frac{\partial T_s}{\partial y} = k_L \frac{\partial T_L}{\partial y}. \quad [5]$$

Here, k_s and k_L represent the thermal conductivities for solid and liquid, respectively. Furthermore, both liquid and solid temperatures must be well behaved everywhere so that

$$\text{as } y \to \infty, \quad T_L(y, t) \quad \text{is finite} \quad [6]$$

and

$$\text{as } y \to -\infty, \quad T_s(y, t) \quad \text{is finite.} \quad [7]$$

The solution for the liquid temperature distribution in dimensionless terms with reference to the temperature of the superheated liquid is

$$\Theta_L(\eta, \tau) = \left[\operatorname{erf}\left(\frac{\eta}{\sqrt{\tau - 1}}\right) - \operatorname{erf}\left(\frac{\eta}{\sqrt{\tau}}\right) - \frac{2}{\pi} \exp\left(\frac{-\eta^2}{\tau}\right) \sum_{n=0}^{\infty} \frac{(-1)^n H_{2n}\left(\frac{\eta}{\sqrt{\tau}}\right)}{n! 2^{2n} (2n + 1)(\sqrt{\tau})^{2n+1}}\right], \quad [8]$$

where H_{2n} is the Hermite polynomial, and where

$$\eta \equiv \frac{y}{2\sqrt{\alpha_L t_g}} \quad [9]$$

and

$$\tau \equiv \frac{t + t_g}{t_g} \quad [10]$$

and the dimensionless temperature is defined as

$$\Theta_L(\eta, \tau) \equiv \left(\frac{T_L(y, t) - T_{sup}}{T_{sup} - T_{sat}}\right)\left[1 + \sqrt{\frac{(k\varrho C)_L}{(k\varrho C)_s}}\right]. \quad [11]$$

The parameters ϱ and C are density and specific heat, respectively. The transient temperature distribution is shown in figure 3(a). Note that by the choice of parameters, the different combinations of material properties are automatically accounted for without a change in the dimensionless temperature profiles. As time progresses, the dimensionless temperature $\Theta_L(\eta, \tau)$, which is negative, vanishes and thus represents the degree to which the thermal boundary layer has been depressed from uniform superheat.

The contact-line (wall) temperature time behavior is obtained from [8] by letting the distance from the wall, y, vanish to obtain

$$\Theta_w(\tau) \equiv \Theta_L(0, \tau) = -\frac{2}{\pi} \sum_{n=0}^{\infty} \frac{(2n)!}{(n!)^2 2^{2n} (2n + 1)(\sqrt{\tau})^{2n+1}}. \quad [12]$$

With increased dwell time the contact-line temperature [figure 3(b)] increases back toward the superheat temperature. At some point, this temperature will be sufficiently large to sustain stable nucleation at a given cavity.

Using the Clausius–Clapeyron equation, the saturation temperature corresponding to the local inside pressure of a bubble with a radius R_c is given by

$$\Theta_{RC} = \left(\frac{2\sigma T_{sat}}{\varrho_G \Delta i_{FG} R_c \Delta T_{sup}} - 1\right)\left[1 + \sqrt{\frac{(k\varrho C)_L}{(k\varrho C)_s}}\right], \qquad [13]$$

with ϱ_G the vapor density and Δi_{FG} is the latent heat. Following Hsu (1962), the expression for the minimum active cavity size comes directly from the Laplace equation for a metastable bubble which, when combined with the Clausius–Clapeyron equation, yields

$$R^*_{c,min} = \frac{R_{c,min} \Delta i_{FG} \Delta T_{sup}}{2\sigma T_{sat} \upsilon_{FG}}. \qquad [14]$$

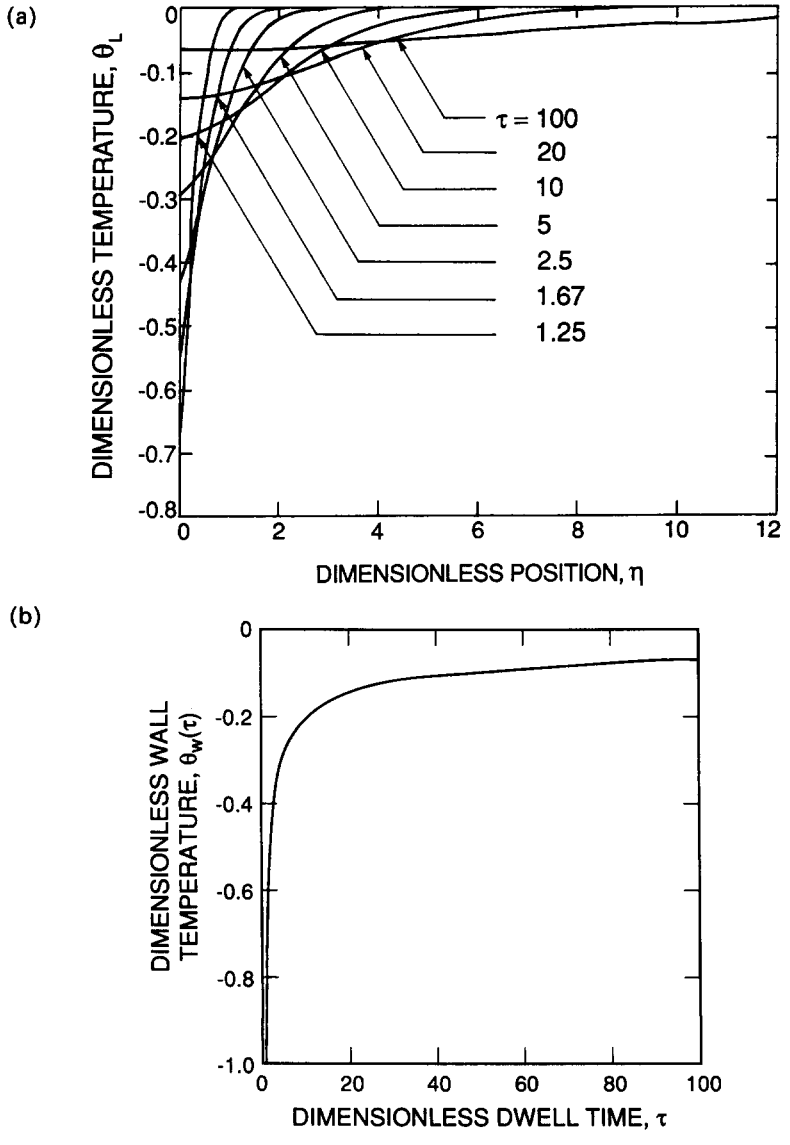

Figure 3. Dimensionless liquid temperature profiles and contact-line temperature during the waiting period; (a) liquid temperature; (b) contact-line temperature.

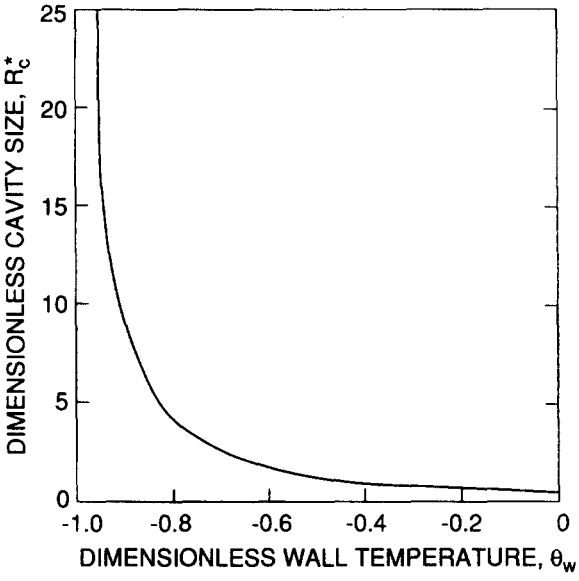

Figure 4. Minimum active cavity size as a function of wall temperature.

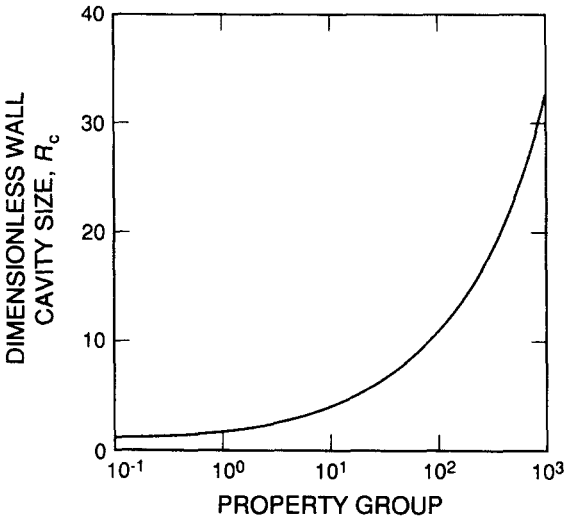

Figure 5. Figure-of-merit for nucleating surfaces. Maximum value of the minimum active cavity size.

The surface tension between the liquid and vapor is given by σ and the specific volume of vaporization is v_{FG}. Equations [13] and [14] are combined to give

$$R^*_{c,min} = \left\{1 + \Theta_w(\tau)\left[1 + \sqrt{\frac{(k\varrho C)_L}{(k\varrho C)_s}}\right]^{-1}\right\}^{-1}. \quad [15]$$

This stability criterion is shown in figure 4. As the waiting time increases, Θ_w vanishes and the minimum active cavity size approaches that associated with the uniform superheat. As the dwell time vanishes, Θ_w approaches its limiting value of negative unity and only large cavities can nucleate since the wall superheat would be a minimum.

The difficulty in this analysis, of course, is identical to the difficulty in previous stability criteria developed for boiling. While this procedure is useful in qualitatively explaining observations, it requires quantitative information about the nucleating surface characteristics to be useful. This is the subject of the next section.

Figure-of-merit

Actual determination of the nucleation site density, even if possible, is patently impractical. An alternate approach would be to find a reasonable "figure-of-merit" which would be sufficiently definitive to allow analysis to proceed.

While there is no theoretical basis for a minimum energy principle for nucleation at cavities, it may be that preferential nucleation might take place at cavities in a way whereby the surface energy for production is minimized. If this were to be the case, nucleation would favor the maximum cavity size which will produce stable cavities.

A figure-of-merit for the system is thus obtained by considering the surface to be made up only of cavities producing the largest stable nuclei—those for which the dwell time vanishes and the wall temperature is at its minimum value. Letting the waiting time vanish so that $\Theta_w = -1$ yields the maximum value of the minimum active cavity size from [15] as

$$\text{Max}(R^*_{c,min}) = \left\{1 - \left[1 + \sqrt{\frac{(k\varrho C)_L}{(k\varrho C)_s}}\right]^{-1}\right\}^{-1}, \quad [16]$$

which is shown in figure 5. Having assumed the surface to be made up of cavities of this (fictitious) size, one could proceed to calculate the needed quantities such as growth times, departure sizes and nucleation frequencies, and see if the results proved useful. By considering this figure-of-merit, the dwell time between bubbles has been neglected. Therefore, calculation of the growth rate through

standard methods, coupled with a departure size criterion, will then yield the nucleation frequency at a given site, this frequency being a maximum value.

Bubble Departure Size

By balancing drag and surface tension forces, the departure radius of a bubble is given by

$$R_d = K\sqrt{\frac{4\sigma R_c}{C_D \varrho_L w_{LB}^2}}, \qquad [17]$$

where K accounts for, among other things, the fraction of the surface tension forces acting in opposition to the drag and w_{LB} is the average axial velocity over the bubble producing a drag coefficient C_D. It is assumed that all the bubbles grow entirely within the viscous sublayer. (This assumption has been confirmed by the result.) The average velocity is given by

$$w_{LB} = \frac{1}{2R_d}\int_0^{2R_d}\left(\frac{\tau_w y}{\mu}\right)dy = \frac{\tau_w R_d}{\mu}, \qquad [18]$$

where τ_w is the wall shear stress and μ is the liquid viscosity. The normal turbulent friction coefficient (Schlichting 1979) is used to calculate the wall shear stress with the corresponding friction coefficient given by

$$C_f \equiv \frac{2\tau_w}{\varrho_L w_L^2} = 0.0791\ \mathrm{Re}_D^{-1/4}; \qquad [19]$$

Re_D is the local Reynolds number based on the duct diameter, D, and w_L is the local mean flow velocity. This assumption will underestimate the wall shear in nozzles where the duct convergence suppresses the boundary layer, thereby steepening the gradients. This will lead to late departure estimates and underestimated frequencies, tending somewhat to offset the vanishing dwell-time estimate. Of course, the estimate will be reasonably accurate with straight ducts. The departure size thus becomes

$$R_d = \sqrt{\left(\frac{K\mu}{\tau_w}\right)\sqrt{\frac{4\sigma R_c}{C_D \varrho_L}}}, \qquad [20]$$

with ϱ_L the liquid density. The drag coefficient is taken to be (Schlichting 1979)

$$C_D = \begin{cases} \dfrac{24}{\mathrm{Re}_B} & \mathrm{Re}_B < 1 \\ 18.5\ \mathrm{Re}_B^{-0.6} & 1 \leqslant \mathrm{Re}_B < 500 \\ 0.44 & 500 \leqslant \mathrm{Re}_B < 2\times 10^5 \end{cases} \qquad [21]$$

where Re_B is the local bubble Reynolds number based on w_L. The departure size in dimensionless terms thus becomes

$$R_d = 0.5787K^{5/7}\left[\left(\frac{\sigma R_c}{\varrho_L}\right)^{1/2}\left(\frac{\mu_L}{\tau_w}\right)^{7/10}\left(\frac{1}{\nu_L}\right)^{3/10}\right]^{5/7}, \qquad [22]$$

which can be nondimensionalized to yield

$$R_d^* \equiv \frac{R_d}{R_c} = \frac{0.818}{\sqrt{C_f}}\left(\frac{K^2}{\mathrm{We}_{cL}}\right)^{5/14}\left(\frac{1}{\mathrm{Re}_{cL}}\right)^{2/7}. \qquad [23]$$

Both the Weber and Reynolds numbers are based on the mean flow velocity and the cavity size. Thus, $\mathrm{We}_{cL} = \varrho_L R_c w_L^2/\sigma$ and $\mathrm{Re}_{cL} = R_c w_L/\nu_L$. Recall that K accounts for the fraction of the surface tension force which opposes the drag at departure. It is arbitrarily taken as unity in what follows.

The available data on flashing in pipes and nozzles (Abuaf *et al.* 1981; Reocreux 1976; Brown 1961; Celata *et al.* 1982; Wu *et al.* 1981; Sozzi & Sutherland 1975; Bailey 1951; Ardron & Ackerman 1978) were examined and departure sizes calculated using [22] with $K = 1$. For all these data, departure sizes calculated to be in the range 1–100 mm were obtained. The smallest values correspond to the highest flows and largest superheats near 100°C as expected. In all cases, the values of departure size calculated were approximately equal to or larger than the given value of $\mathrm{Max}\{R_{c,\min}\}$.

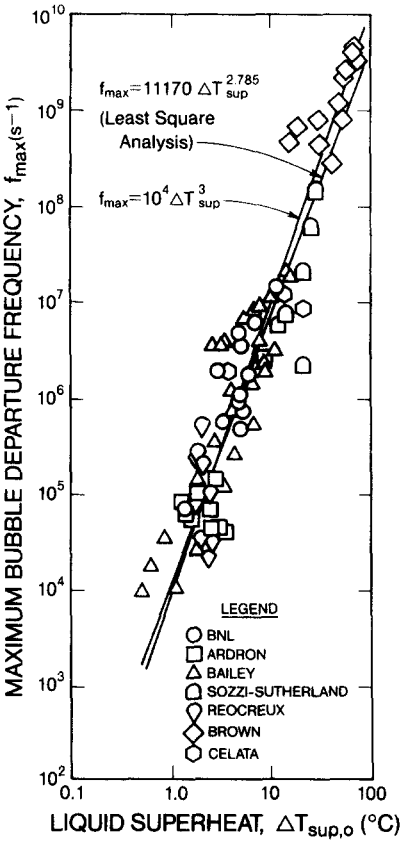

Figure 6. Correlation of throat bubble departure frequencies for "figure-of-merit" cavities.

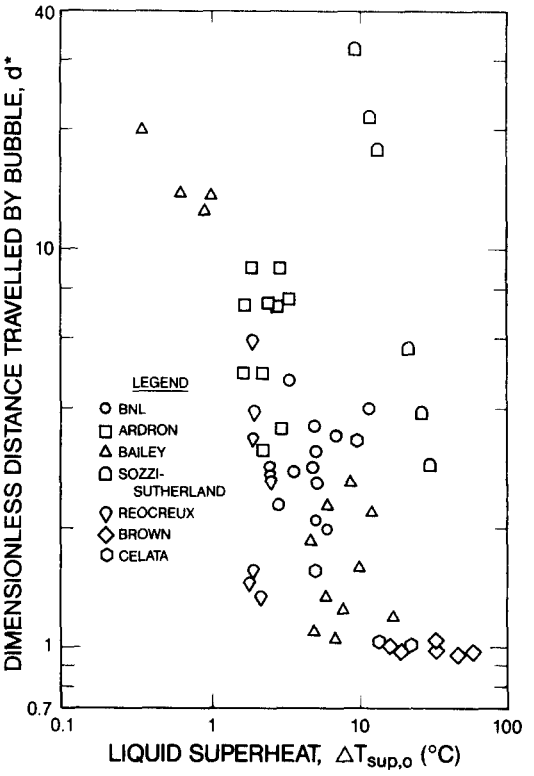

Figure 7. Distance traveled by one departing bubble in one nucleation period relative to the departure diameter.

Bubble Nucleation Frequency

For wall nucleation conditions, the nucleation frequency per site and the site density are the quantities which describes the system nucleation behavior. The cavity size distribution in the nozzle should be characterized by that in the throat where the superheat and nucleation frequency is at a maximum. Thus, the frequency in the throat will be determined and then used to obtain the site density. The latter will then be used for the balance of the nozzle.

The data which exist in the literature (Abuaf *et al.* 1981; Reocreux 1974; Brown 1961; Celata *et al.* 1982; Wu *et al.* 1981; Sozzi & Sutherland 1975; Bailey 1951; Ardron & Ackerman 1978; Reocreux† 1976) were used to calculate the nucleation frequency for the figure-of-merit cavities (assumed size). Growth rates were assumed to be thermal-diffusion-controlled (Plesset & Zwick 1954) rates. The results are shown in figure 6. The liquid superheats span the range from <1°C to close to 100°C. A reasonable fit close to the least-squares condition of these data was found to yield a maximum nucleation frequency of

$$f_{max} = 10^4 \Delta T_{sup}^3, \qquad [24]$$

with ΔT_{sup} in degrees Kelvin and frequency in hertz so that the coefficient has units of Hz/K^3 or $s^{-1}K^{-3}$. Frequencies close to $10^{10}\ s^{-1}$ were calculated at the largest values of superheat near 100°C. These are unexpectedly large values characteristic of what one normally would expect at the lower bound for homogeneous nucleation. In spite of the fact that these are artificial values, it is seen in figure 7 that the ratio of the distance traveled in one period after departure, w_L/f_{max}, to the bubble

†Note that the experiments of Reocreux had a uniform-diameter inlet length with friction-dominated pressure gradient in the single-phase zone up to the saturation zone followed by a flashing zone to a location termed the "col" where the pipe diverged. This divergence point is herein termed the throat to be consistent with nozzle nomenclature.

size at departure, $2R_d$, is generally above unity. In only two cases is this ratio below unity, having values of 0.9 and 0.95 respectively, well within the accuracy of the calculation of R_d.

The correlation for nucleation frequency is dimensional, a somewhat undesirable situation. However, at this time no dimensionless method of correlating the data has been found to produce results as well correlated as that shown.

Maximum Local Wall Nucleation Rate and Nucleation Site Density

It is typical of rapidly nucleating systems that the process of nucleation itself can turn off the nucleation process due to the energy absorbed or liberated by the formation of the nuclei (Wegener 1969, 1975). Thus, it is expected that with sufficiently rapid nucleation, the available superheat in the nucleation layer will be consumed. In order to calculate a maximum wall nucleation rate for each set of data, the nucleation site surface density can be calculated as

$$N_{ns}^* \equiv (2R_d)^2 N_{ns} = \frac{(2R_d)^2 J_{w\max} A_c}{f_{\max} \xi}, \qquad [25]$$

where $J_{w\max}$ is the maximum wall nucleation density which must be determined, A_c is the local cross-sectional area of the nozzle and ξ is the local perimeter. Considering the nucleation wall layer, a convective energy balance yields

$$J_{w\max} = \frac{3\varrho_L C_L v_{FG}}{\Delta i_{FG} \pi R_N^2(z) R_c^3} \frac{d}{dz}\left[R_N(z) \Delta T_{sup}(z) \int_0^\delta w(y)\, dy \right], \qquad [26]$$

where δ is the thickness of a thin cylindrical disk of liquid of radius equal to the cavity radius having the mass of the nuclei, R_N is the local nozzle radius and z is the axial coordinate. Thus, considering the nucleated bubble as a hemisphere of radius equal to the cavity radius:

$$\delta = \tfrac{2}{3} R_c \left(\frac{\varrho_G}{\varrho_L} \right). \qquad [27]$$

The velocity in [26] is obtained from the universal velocity profile over the thickness δ (Schlichting 1979).

Equation [26] must, of course, be evaluated for each given geometry. For pipe flow, $R(z)$ is fixed and the evaluation is relatively straightforward. For the case of a nozzle where the radius varies linearly between R_1 at the inlet and R_2 at the throat, and where the acceleration pressure profile in the nucleation zone can be approximately linearized, it is found that the wall nucleation rate is

$$J_{w\max} = 2.94 \times 10^{-3} \left(\frac{C_L \dot{m}^{7/4}}{\sigma \mu^{3/4} T_{sat}} \right) \left(\frac{\varrho_G \Delta T_{sup,t}}{\varrho_L L_n} \right)^2 \frac{z}{R_N^{19/4}(z)} \left[1 - 2.75 \left(\frac{\Delta R}{R} \right) \left(\frac{z}{L_N} \right) \right], \qquad [28]$$

where z is the distance from saturation ($0 < z < L_n$), L_n is the length of the nucleation zone, L_N is the length of the nozzle, $\Delta T_{sup,t}$ is the superheat at the throat and $\dot{m}$ is the flow rate. This equation can be nondimensionalized to yield

$$J_{w\max}^* \equiv \frac{J_{w\max} R^4}{w_L} = 1.296 \times 10^2 \left(\frac{\varrho_v}{\varrho_L} \right)^2 H^*(z) \frac{\varrho_L C_L \Delta T_{sup,t}^2 R_N^3}{\sigma T_{sat} L_N^2} \mathrm{Re}_D^{3/4}, \qquad [29]$$

where the Reynolds number is the local value based on the flow rate and nozzle diameter. The geometric function is given for the nozzle radius $R_N = R_N(z)$ as

$$H^*(z) = \frac{z}{R_N} \left[1 - 2.75 \left(\frac{\Delta R}{R_N} \right) \left(\frac{z}{L_N} \right) \right], \qquad [30]$$

with ΔR the radius difference between the inlet and outlet.

Values for the dimensionless nucleation site density can be obtained from the experimental data cited previously. The dimensionless nucleation site density is shown in figure 8 and is well-correlated by the ratio of the local superheat-related cavity size, R_{cs}, to the bubble departure size, R_d, as

$$N_{ns}^* = 10^{-7} R_c^{*-4}, \qquad [31]$$

where $R_c^* = R_{cs}/R_d$. The least-square coefficient and exponent were 1.039×10^{-7} and -3.8,

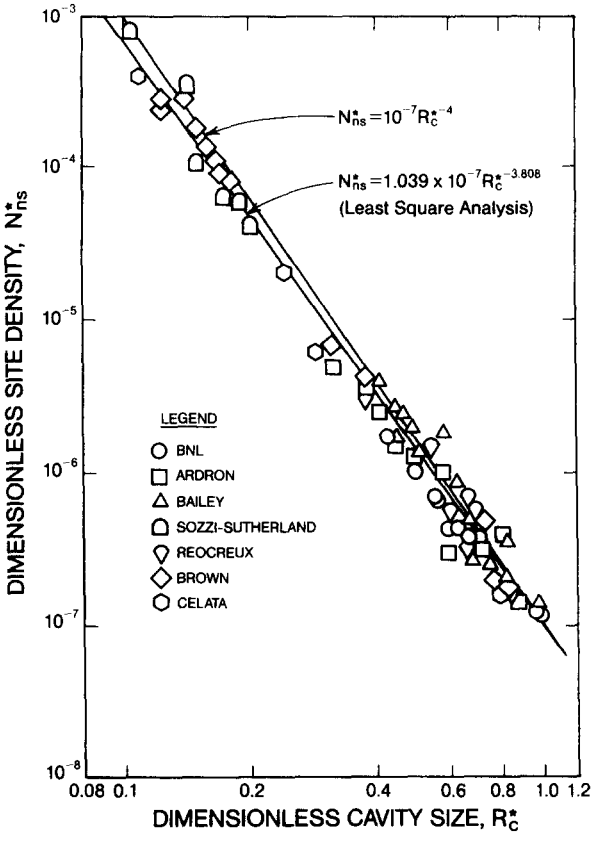

Figure 8. Correlation of dimensionless nucleation site density.

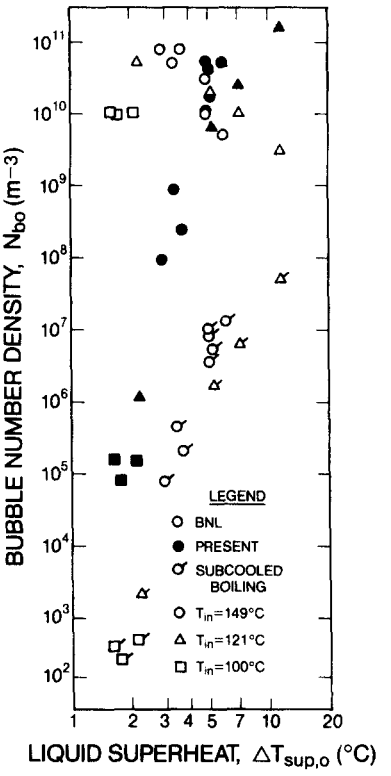

Figure 9. Comparison of calculated bubble number densities at the nozzle throat with other predictions.

respectively. Equation [31] shows the density of active nucleation sites to be proportional to the square of the departure size and inversely dependent on the fourth power of the superheat-related cavity size. The nucleation site density is thus proportional to the superheat to the power of 4. Thus, both thermodynamic and hydrodynamic states are important. Increasing the local velocity decreases the departure size and snuffs out active sites, in accordance with the observations of Bergles & Rohsenow (1962) for subcooled boiling. An increase in frequency at the remaining active sites would thus occur with decreasing pressure, increasing superheat and increasing velocity.

It is interesting to compare [31] with that proposed by Kocamustafaogullari & Ishii (1983) in similar form as

$$N^*_{ns} = f(\varrho^*)R^{*-4.4}_c \quad \text{for subcooled boiling,} \qquad [32]$$

where

$$f(\varrho^*) = 2.157\times10^{-7}\varrho^{*-3.2}(1+0.0049\varrho^*)^{4.13} \qquad [33]$$

with

$$\varrho^* \equiv \frac{\Delta\varrho}{\varrho_G}. \qquad [34]$$

Typical values of the function of density are 8.3×10^{-14}, 4.6×10^{-13} and 1.7×10^{-10} for density ratios of 1000, 100 and 10, respectively. Thus, even with similar superheat behavior, the major differences are due to the coefficient. It is evident why the subcooled boiling formulation does not work for flashing.

Bubble Number Density at the Throat

It is reasonable to expect that the nucleation site density at the throat is characteristic of the rest of the nucleation zone. The bubble number density at the throat may thus be determined by approximate integration of the bubble transport equation as

$$N_{B,t} \cong \frac{1}{w_{B,t} A_{c,t}} \int_0^{L_n} N_{ns}(z) f_{max}(z) \xi(z)\, dz, \qquad [35]$$

with w_B the bubble velocity. The results are shown in figure 9 in comparison with the estimates provided by Wu *et al.* (1981) on the basis of an assumed inception void fraction. Furthermore, the values predicted by the subcooled boiling model of Kocamustafaogullari & Ishii (1983), developed for subcooled boiling only, are also shown in the figure to be several orders lower than those predicted herein, and indicate why this model did not predict results well for nozzles. It can thus be seen that flashing and subcooled boiling are both quantitatively and qualitatively different in their basic mechanisms, and correlations developed for one should not be used arbitrarily for the other.

Throat Superheat

The wall nucleation rate may be written in terms of the nucleation site density and site frequency as

$$J_{w\,max} = \frac{N_{ns} f_{max} \xi}{A_c}. \qquad [36]$$

From this point on, any terms involving the nucleation frequency must be dimensional in nature due to the dimensionality of [24]. Recalling the expression for departure size, and using the cavity size in terms of the superheat through the Clausius–Clapeyron equation, the throat superheat is obtained as

$$\Delta T_{sup,t} = \left(\frac{J_{w\,max} A_c}{B\xi} \right)^{7/44}, \qquad [37]$$

where the dimensional coefficient B is given by

$$B = 1.673 \times 10^{-4} R_c^{9/7} \left(\frac{\varrho_G \Delta i_{FG}}{2\sigma T_{sat}} \right)^{23/7} \frac{1}{C_f We_{cL}^{5/7} Re_{cL}^{4/7}} \qquad [38]$$

with SI units (m, kg, s) consistent with [37]. The coefficient 1.673×10^{-4} has units of $s^{-1} K^{-3}$, consistent with the coefficient in the frequency equation given by [24]. A comparison between the calculated and observed values is shown in figure 10. The standard deviation is 1.9°C, indicating a reasonable accuracy in the calculation.

Void Development to the Throat

The void fraction at the throat may be found by integrating the vapor continuity equation to obtain

$$\epsilon_t = \frac{1}{\varrho_G w_{B,t}} \int_0^{z_0} \Gamma_V(z)\, dz. \qquad [39]$$

where the subscript "0" indicates, as before, the throat conditions. The volumetric vapor generation rate is given as (Zuber *et al.* 1966)

$$\Gamma_V = \frac{d}{dz} \left(\frac{1}{A_c} \int_0^z m_B(z, z') J_w(z') \xi(z')\, dz' \right), \qquad [40]$$

where $m_B(z, z')$ is the mass of a bubble at z which was nucleated at z'. The mass of the bubble at any location may be determined through the departure size at the nucleation site given by [22], and an analysis for bubble growth in a variable pressure field (Jones & Zuber 1978).

4. RESULTS AND DISCUSSION

Void Development to the Throat

In virtually all previous flashing models, the nucleation zone is treated as a single point of flashing inception. This has been previously justified since the zone of supersaturation in many cases, such as those with rapidly converging nozzles, is quite narrow. However, in this zone, the voids which develop from the nuclei form the basis for interfacial mass transfer and subsequent growth downstream. In other cases, such as constant-area flows with friction-dominated pressure profiles, this is not the case. It is, therefore, important that both the size and number be determined locally so that accurate calculations of void development may be undertaken.

Calculations were made for all runs in the previously referenced data sets (Abuaf *et al.* 1981; Reocreux 1974, 1976; Brown 1961; Celata *et al.* 1982; Wu *et al.* 1981; Sozzi & Sutherland 1975; Bailey 1951; Ardron & Ackerman 1978), which comprised all the subcooled-inlet, critical flow, nozzle data available. All had similar behavior. The smallest throat void fraction (figure 11) was computed for Ardron & Ackerman's Run C25, having a throat superheat of 1.66 K with 1.6 bar inlet pressure. While the nucleation site density shown in figure 12 increased to approx. 140 m^{-2} with overall wall nucleation rates of about $5 \times 10^8\ m^{-3}s^{-1}$ (bulk equivalent), the throat void fraction was only 10^{-5}.

The largest throat void fraction of 0.9% was calculated for Brown's (1961) Run 39, shown in figure 13, having a throat superheat of 81.6 K, an inlet pressure of 68.4 bar and a wall nucleation rate at the throat of $3 \times 10^{23}\ m^{-3}\ s^{-1}$ (figure 14). This was 15 orders of magnitude larger than the nucleation rate found for Ardron & Ackerman (1978). Note that the throat superheat of 81.6 K represents a pressure undershoot of almost 59 bar.

Where measurements of void fraction exist, the agreement was within the experimental accuracy of the experiment. This, however, is no real test, since the data are usually accurate to within 1–2% voids at best and the computed maximum throat void fraction when data existed was on the order of 6×10^{-5}. Nevertheless, the calculations and existing data support the original hypothesis of Abuaf *et al.* (1983) that flashing flows with a subcooled inlet had virtually all single-phase flow upstream of the restriction or throat.

Critical Mass Flows

The work described above shows that negligible voids exist at the throat for flashing of initially subcooled liquids and supports the original hypothesis of Abuaf *et al.* (1983). Single-phase theory

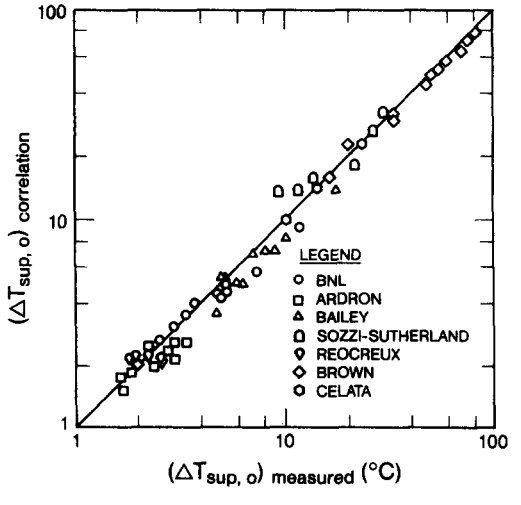

Figure 10. Comparison of calculated and measured throat superheats.

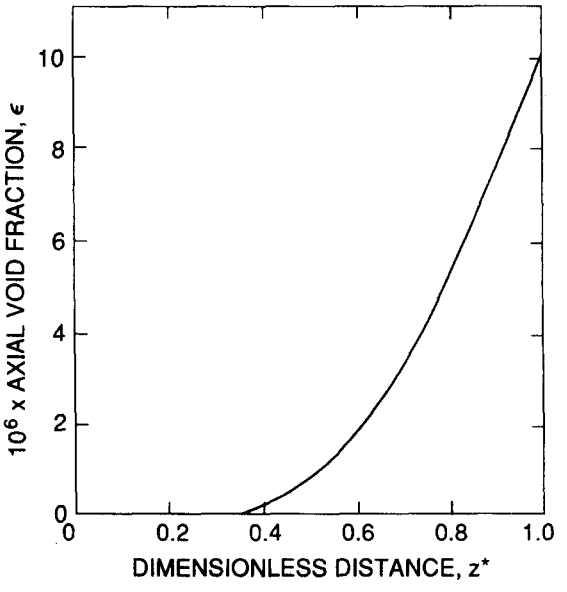

Figure 11. Void development for Run C35 of Ardron & Ackerman (1978).

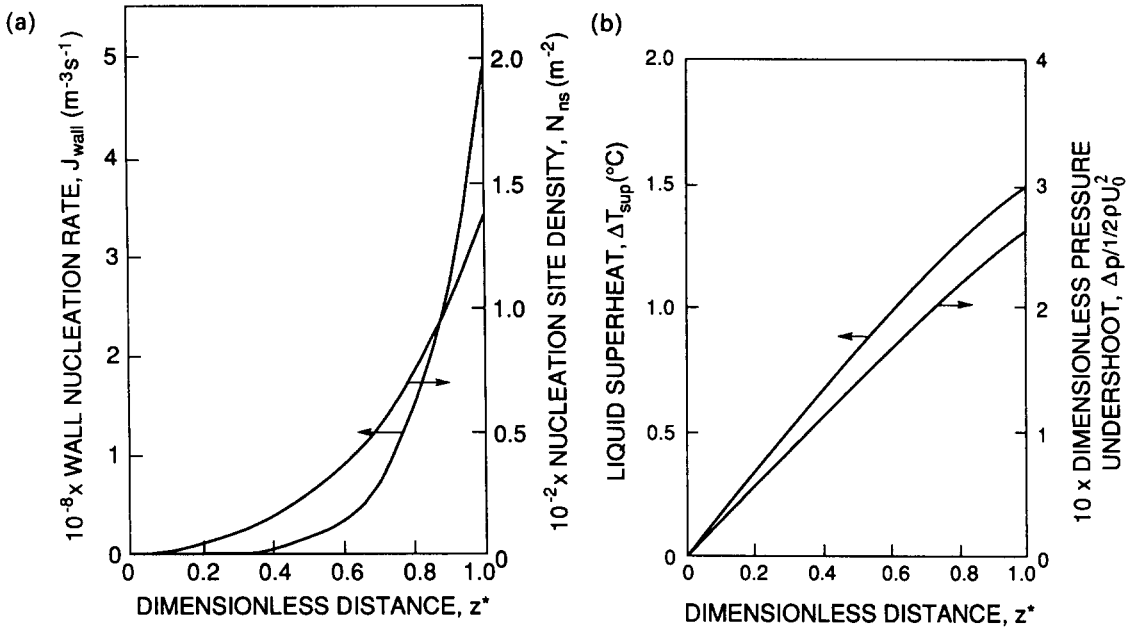

Figure 12. Calculations for the nucleation zone for the conditions of Run C35 of Ardron & Ackerman (1978). Conditions for this data set: $T_{in} = 111.5$°C, $p_{in} = 1.59$ bar, $G = 7740$ kg/m^2 s, $\Delta T_{sup,0} = 1.66$ K. (a) Wall nucleation rate and nucleation site density; (b) liquid superheat and pressure undershoot.

may thus be used to calculate flow rates under such conditions, where the correct throat pressure must be obtained from the calculation of the throat superheat, [30]. Note, however, that these calculations are not of critical flow, but of the flow rate under critical flow conditions. In the absence of experimental evidence, one would still have to obtain an independent estimate of the choked flow condition in order to predict the throat superheat and thus the flow rate. However, this work shows that there is a correspondence between the two which can provide an important independent check of the critical flow condition.

The result of these calculations is shown in figure 15 for the data cited previously. The standard deviation between the predicted and measured critical flow rates is approx. 3%, a 40% improvement over earlier work (Abuaf *et al.* 1983) where 5% accuracy was obtained using the pressure undershoot correlation of Jones (1980).

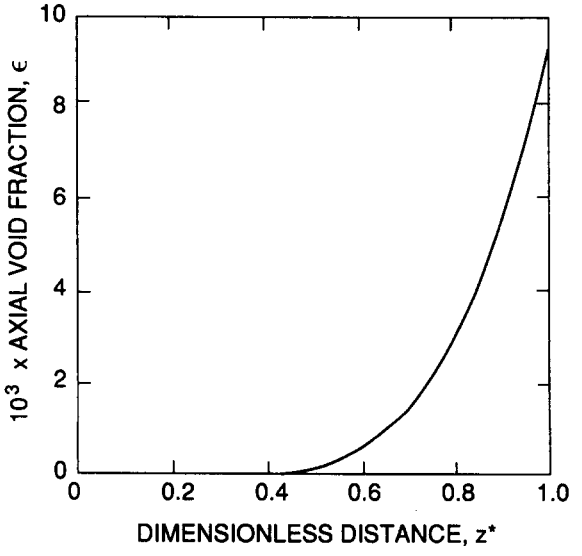

Figure 13. Void development for Run 39 of Brown (1961).

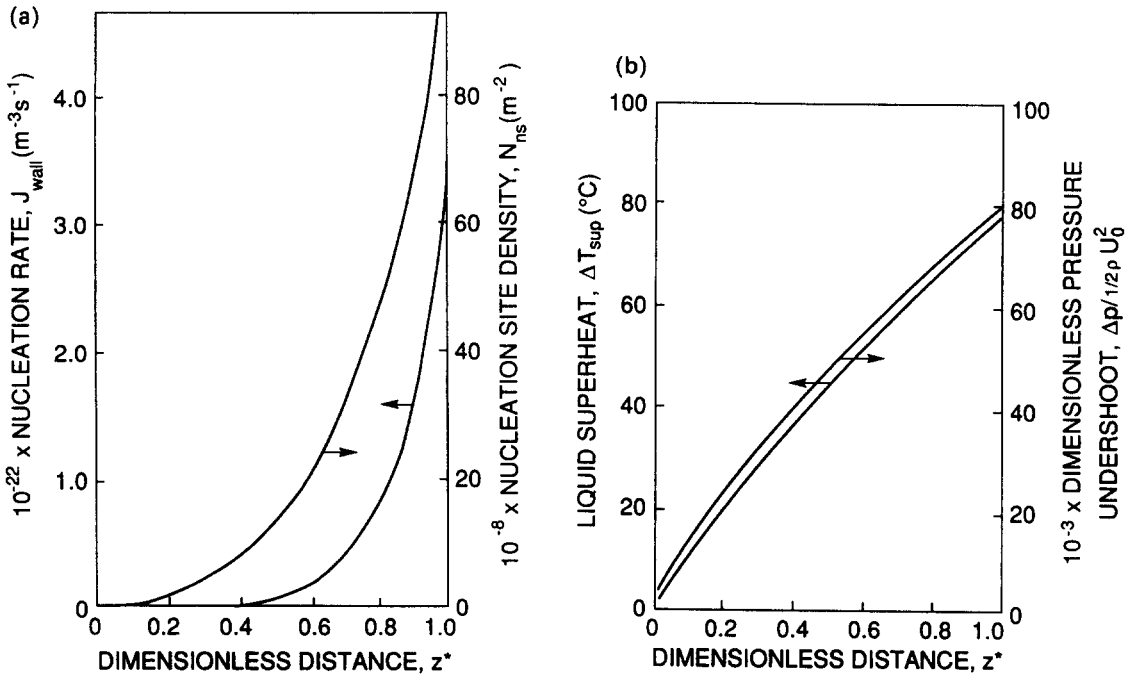

Figure 14. Calculations for the nucleation zone for the conditions of Run 39 of Brown (1961). Conditions for this data set: $T_{in} = 280°C$, $p_{in} = 68.4$ bar, $G = 303$ kg/m^2 s, $\Delta T_{sup,0} = 81.6$ K. (a) Wall nucleation rate and nucleation site density; (b) liquid superheat and pressure undershoot.

5. CONCLUSIONS AND RECOMMENDATIONS

A distributed model for nucleation in the superheated zone upstream of the throat in nozzles during flashing has been described which has the following features:

1. Development of a stability criterion for active cavities.
2. Selection of a figure-of-merit for a nucleating surface which ties the stability criteria to an obtainable nucleation site density and cavity nucleation frequency in flashing flows.
3. Calculation of the departure size of nuclei in the nucleation zone.
4. Correlation of nucleation frequencies at a given site and the surface density of nucleation sites as determined from the existing data.
5. Determination of the maximum, energy-limited rate of nucleation.

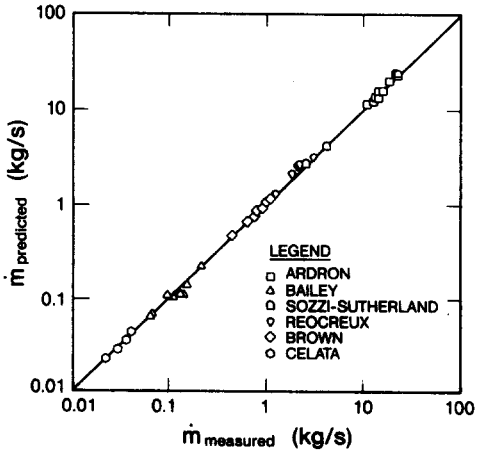

Figure 15. Comparison of calculated and measured critical flow rates.

Utilization of the nucleation model then allows the throat superheat to be calculated within 2% for the existing data over the approximate range from <1 K to nearly 100 K. The range of data include pressures to almost 70 bar, and expansion rates from 0.2 bar/s to over 1 Mbar/s, extending existing methods by 4 orders of magnitude.

Nucleation site density was correlated from the data and found to vary approximately with superheat to the 4th power of the superheat, somewhat lower than that proposed earlier by Kocamustafaogullari & Ishii (1983) for subcooled boiling but similar, their power being 4.4. While the nucleation site density behavior with superheat is quite similar in both cases, the actual magnitudes are much different due to their functionality with density. The resultant magnitudes of the bubble number densities in the case of flashing were found to be orders-of-magnitude larger than those computed for subcooled boiling.

Bubble sizes at departure upstream of the throat were calculated to be in the range 1–100 mm and were not constant as has been heretofore assumed by many. Nucleation rates at the throat were also variable and were calculated to span the range 10^8–10^{23} $m^{-3}\,s^{-1}$. The resultant calculations of throat number densities in all cases ranged between $\sim 10^8$ and 10^{11} m^{-3}.

Bubble transport calculations show that even for the cases with the largest superheat and highest bulk-equivalent nucleation rates, near 100 K and over 10^{23} $m^{-3}\,s^{-1}$, negligible ($<1\%$) voids exist at the throat, confirming the previous hypotheses of Abuaf *et al.* (1980, 1983). A result of this confirmation is that calculations of subcooled-inlet flow rates by single-phase methods agree within 3% of the critical flows measured once the correct throat superheat (and thus pressure) is obtained.

The differences accounted for by the methods described herein represent throat pressure undershoots up to the order of 60 bar! This large correction, coupled with the realization that the throat conditions are essentially single-phase liquid, was the major factor in developing an ability to calculate the critical mass flow rates accurately for all data. As shall be seen in the companion paper (Blinkov *et al.* 1993), the ability to determine both the number density and the size of the initial nuclei is also the key to accurately calculating void development downstream of the nucleation zone.

Finally, the methods described herein provide the first method of relating the fundamental thermophysical theory of surface nucleation to the prediction of global quantities. While heuristic, this method allows the determination of nucleation site densities from a knowledge of the local superheats, thereby relating cavity nucleation theory to such global quantities such as liquid superheat, bubble number density, mass flow rates and void fraction.

REFERENCES

ABDOLLAHIAN, D., HEALZER, J., JANSSEN, E. & AMOS, C. 1982 Critical flow data review & analysis. Report EPRI NP-2192.

ABUAF, N., JONES, O. C. JR & WU, B. J. C. 1980 Critical flashing flow in nozzles with subcooled inlet conditions. In *Polyphase Flow and Transport Technology* (Edited by BAJURA, R. A.), pp. 65–74. ASME, New York.

ABUAF, N., ZIMMER, G. A. & WU, B. J. C. 1981 A study of nonequilibrium flashing of water in a converging–diverging nozzle, Vol. 1—Experimental. Reports NUREG/CR-1864 & BNL-NUREG-51317.

ABUAF, N., JONES, O. C. JR & WU, B. J. C. 1983 Critical flashing flow in nozzles with subcooled inlet conditions. *Trans. ASME Jl Heat Transfer* **105,** 379–383.

AGUILAR, F. & THOMPSON, S. 1981 Nonequilibrium flashing model for rapid pressure transient. ASME preprint, Paper No. 81-HT-35.

ALAMGIR, M. D. & LIENHARD, J. H. 1981 Correlation of pressure undershoot during hot-water depressurization. *Trans. ASME Jl Heat Transfer* **103,** 52–55.

ARDRON, K. H. 1978 A two-fluid model for critical vapor–liquid flow. *Int. J. Multiphase Flow* **4,** 323–337.

ARDRON, K. H. & ACKERMAN, M. C. 1978 Studies of the critical flow of subcooled water in a pipe. In *Proc. 2nd CSNI Specialist Mtg*, Paris, pp. 517–543.

BAILEY, J. F. 1951 Metastable flow of saturated water. *Trans. ASME* **73,** 1109–1116.

BANKOFF, S. G. 1958 Entrapment of gas in the spreading of a liquid over a rough surface. *AIChE Jl* **4,** 24–26.

BAUER, E. G., HOUDAYER, G. R. & SUREAU, H. M. 1976 A nonequilibrium axial flow model and application to LOCA analysis: the CLYSTERE system code. Presented at the *OECD/NEA Specialists' Mtg on Transient Two-Phase Flow*, Toronto, Ontario.

BERGLES, A. E. & ROHSENOW, W. M. 1962 Forced convective surface boiling heat transfer and burnout in tubes of small diameter. MIT Report 8767-21.

BLINKOV, V., JONES, O. C. & NIGMATULIN, B. I. 1993 Nucleation and flashing in nozzles—2. Comparison with experiments using a five-equation model for vapor void development. *Int. J. Multiphase Flow* **19,** 965–986.

BROWN, R. A. 1961 Flashing expansion of water through a converging—diverging nozzle. M.S. Thesis, Univ. of California, Berkeley CA. UKAEC Report UCRL-6665-T.

CELATA, C. P., CUMO, M., FARELLO, G. E. & INCALCATERRA, P. C. 1982 Critical flow of subcooled liquid and jet forces. Report ENEA-RT/INC(8218).

CLARK, H. B., STRENGE, P. S. & WESTWATER, J. W. 1965 Active sites for nucleate boiling. *Chem. Engng Prog. Symp. Ser.* **61,** 103–110.

COLLINS, R. L. 1980 Choked expansion of subcooled water and I.H.E. flow model. *Trans. ASME Jl Heat Transfer* **100,** 275–280.

EDWARDS, A. R. 1968 Conduction controlled flashing of a fluid and the prediction of critical flow rates in a one-dimensional system. Report AHSB (S) R-147, UKAEA, AERE.

EPRI 1979 Marviken full scale critical flow tests.

FAUSKE, H. K. 1964 The discharge of saturated water through tubes. Presented at the *7th National Heat Transfer Conf., AIChE–ASME*, Cleveland, OH.

FINCKE, J. R., COLLINS, D. R. & WILSON, M. L. 1981 The effects of grid turbulence on nonequilibrium choked nozzle flow. INEL Report NUREG/CR-1977, EGG-2088.

FORSTER, H. K. & ZUBER, N. 1954 Growth of a vapor bubble in a superheated liquid. *J. Appl. Phys.* **25,** 474–478.

FRITZ, W. 1935 Berechnung des maximal volumens von dampfblasen. *Phys. Z.* **36,** 379–384.

FRITZ, G., RIEBOLD, W. & SCULTZE, W. 1976 Studies on thermodynamic nonequilibrium in flashing flow. Presented at the *OECD/NEA Specialists Mtg on Transient Two-phase Flow*, Toronto, Ontario.

GRIFFITH, P. & WALLIS, J. 1959 The role of surface conditions in nucleat boiling. Presented at the *ASME–AIChE Heat Transfer Conf.*, Storrs, CT, preprint 106.

HAN, D. & GRIFFITH, P. 1965 The mechanisms of heat transfer in nucleat pool boiling. *Int. J. Heat Mass Transfer* **8,** 887–904.

HENDRICKS, R. C., SIMONEAU, R. J. & BARROWS, R. F. 1976 Two-phase choked flow of subcooled oxygen and nitrogen. Report NASA-TN-D-8169.

HENRY, R. E. & FAUSKE, H. K. 1971 The two-phase critical flow of one component mixtures in nozzles, orifices, and short tubes. *Trans. ASME Jl Heat Transfer* **93,** 179–187.

HENRY, R. E., FAUSKE, H. K. & MCCOMAS, S. T. 1970 Two-phase critical flow at low qualities. Part I: experimental. *Nucl. Sci. Engng* **41,** 79–91.

HSU, Y. Y. 1962 On the size range of active nucleation cavities on a heating surface. *Trans. ASME Jl Heat Transfer* **94,** 207–212.

HSU, Y. Y. 1972 Review of critical flow, propagation of pressure pulse, and sonic velocity. Report NASA TND-6814.

HSU, Y. Y. & GRAHAM, R. W. 1961 An analytical and experimental study of the thermal boundary layer and the ebullition cycle in nucleate boiling. Report NASA TN-D-594.

JONES, O. C. JR 1980 Flashing inception in flowing liquids. *Trans. ASME Jl Heat Transfer* **102,** 439–444.

JONES, O. C. JR 1982 Toward a unified approach for thermal nonequilibrium in gas–liquid systems. *Nucl. Engng Des.* **69,** 57–73.

JONES, O. C. JR & SAHA, P. 1977 Nonequilibrium aspects of water reactor safety. In *Thermal Hydraulic Aspects of Nuclear Reactor Safety:* Vol. 1, *Light Water Reactors* (Edited by JONES, O. C. JR & BANKOFF, S. G.). ASME, New York.

JONES, O. C. JR & ZUBER, N. 1978 Bubble growth in variable pressure fields. *Trans. ASME Jl Heat Transfer* **100,** 453–459.

JONES, O. C. JR & SHIN, T. S. 1984 Flashing of initially subcooled liquid in nozzles. Presented at the *1984 Japan–U.S. Semin. on Two-phase Flow Dynamics*, Lake Placid, NY.

JONES, O. C. JR & SHIN, T. S. 1986 An active cavity model for flashing. *Nucl. Engng Des.* **95,** 185–196.

LEVY, S. & ABDOLLAHIAN, D. 1982 Homogeneous nonequilibrium critical flows. *Int. J. Heat Mass Transfer* **25,** 759–778.

KOCAMUSTAFAOGULLARI, G. & ISHII, M. 1983 Interfacial area and nucleation site density in boiling systems. *Int. J. Heat Mass Transfer* **26,** 1377–1387.

MALNES, D. 1975 Critical two-phase flow based on nonequilibrium model. In *Nonequilibrium Two-phase Flow* (Edited by LAHEY, R. T. & WALLIS, G. B.), pp. 11–16. ASME, New York.

MOODY, F. J. 1966 Maximum two-phase vessel blowdown from pipes. *Trans. ASME Jl Heat Transfer* **88,** 285–295.

PLESSET, M. S. & ZWICK, S. A. 1954 The growth of vapor bubbles in superheated liquids. *J. Appl. Phys.* **25,** 493–500.

POWELL, A. W. 1961 Flow of subcooled water through nozzles. Westinghouse Electric Corp. Report WAPD-PT-(V)-90.

REOCREUX, M. 1974 Contribution a l'etude des debits critiques en ecoulement diphasique eau–vapeur. Ph.D. Thesis, Univ. Scientifique et Medicale de Grenoble, France.

REOCREUX, M. 1976 Experimental study of steam–water choked-flow. Presented at the *OECD/NEA Specialists' Mtg on Transient Two-phase Flow*, Toronto, Ontario.

RICHTER, H. J. 1981 Separated two-phase flow model: application to critical two-phase flow. Report EPRI NP-1800.

RIEBOLD, W. L., REOCREUX, M. & JONES, O. C. (Ed.) 1981 Blowdown phase. In *Nuclear Reactor Safety Heat Transfer*, pp. 325–378. Hemisphere/McGraw-Hill, New York.

RIVARD, W. C. & TRAVIS, J. R. 1980 A nonequilibrium vapor production model for critical flow. *Nucl. Sci. Engng* **74,** 40–48.

ROHATGI, U. S. & RESHOTKO, E. 1975 Nonequilibrium one-dimensional two-phase flow in variable area channels. In *Nonequilibrium Two-Phase Flow* (Edited by LAHEY, R. T. & WALLIS, G. B.), pp. 47–54. ASME, New York.

SAHA, P. 1978 Review of two phase steam–water critical flow models with emphasis on thermal nonequilibrium. Reports NUREG/CR 0417 & BNL-NUREG-50907.

SAHA, P., ABUAF, N. & WU, B. J. C. 1981 A nonequilibrium vapor generation model for flashing flows. ASME preprint, Paper No. 81-HT-84.

SCHLICHTING, H. 1979 *Boundary Layer Theory*. McGraw-Hill, New York.

SCHROCK, V. E. & AMOS, C. N. 1984 Two-phase critical flow. In *Proc. Japan–US Semin. in Two-phase Flow Dynamics*, Ohtsu, Japan, Paper G.1.

SCHROCK, V. E., STARKMAN, E. S. & BROWN, R. A. 1977 Flashing flow of initially subcooled water in convergent–divergent nozzles. *Trans. ASME Jl Heat Transfer* **99,** 263–268.

SCRIVEN, L. E. 1959 On the dynamics of phase growth. *Chem. Engng Sci.* **10,** 1–13.

SHIN, T. S. & JONES, O. C. JR 1988 Flashing of initially subcooled liquids in nozzles: 1. A distributed nucleation model for flashing inception and critical flow. In *Proc. 3rd Japan–US Semin. on Two-phase Flow Dynamics*, Ohtsu, Japan, Paper G.3.

SHOUKRI, M. S. M. & JUDD, R. L. 1978 A theoretical model for bubble frequency in nucleate pool boiling including surface effects. Presented at the *6th Int. Heat Transfer Conf.*, Toronto, Ontario.

SIMONEAU, R. J. 1975 Pressure distribution in a converging–diverging nozzle during two-phase choked flow of subcooled nitrogen. In *Nonequilibrium Two-phase Flows* (Edited by LAHEY, R. T. & WALLIS, G. B.), pp. 37–44. ASME, New York.

SIMPSON, H. C. & SILVER, R. S. 1962 Theory of one-dimensional two-phase homogeneous nonequilibrium flow. *Proc. Inst. Mech. Engrs Symp. on Two-phase Flow*, pp. 45–53.

SOZZI, G. L. & SUTHERLAND, W. A. 1975 Critical flow of saturated and subcooled water at high pressure. GE Report NEDO-13418.

WEGENER, P. P. 1969 *Nonequilibrium Flows*. Marcel Dekker, New York.

WEGENER, P. P. 1975 Nonequilibrium flow with condensation. *Acta-Mech.* **21,** 65–91.

WINTERS, W. S. & MERTE, H. 1979 Experiments and nonequilibrium analysis of pipe blowdown. *Nucl. Sci. Engng* **69,** 411–429.

WOLFERT, K. 1976 The simulation of blowdown processes with condensation of thermodynamic nonequilibrium phenomena. Presented at the *OECD/NEA Specialists Mtg on Transient Two-phase Flow*, Toronto, Ontario.

WU, B. J. C., ABUAF, N. & SAHA, P. 1981 A study of nonequilibrium flashing of water in a converging–diverging nozzle, Vol. 2—Modeling. Reports NUREG/CR-1864 & BNL-NUREG-51317.

YANG, J., JONES, O. C. JR & SHIN, T. S. 1986 Limitations in the isentropic homogeneous equilibrium Model. *Nucl. Engng Des.* **95,** 196–206.

ZIMMER, G. A., WU, B. J. C., LEONHARD, W. L., ABUAF, N. & JONES, O. C. JR 1979 Pressure and void distributions in a converging–diverging nozzle with nonequilibrium water vapor generation. Report BNL-NUREG-26003.

ZUBER, N. 1963 Nucleate boiling—the region of isolated bubbles: similarity with natural convection. *Int. J. Heat Mass Transfer* **6,** 53–78.

ZUBER, N., STAUB, F. W. & BIJWAARD, G. 1966 Vapor void fraction in subcooled boiling and in saturated boiling systems. *Proc. 3rd Int. Heat Transfer Conf.* **V,** 25–38.